Random walks and NMR measurements in porous media

1993 J. Phys. A: Math. Gen. 26 3349

(http://iopscience.iop.org/0305-4470/26/14/005)

J. Phys. A: Math. Gen. 26 (1993) 3349–3367. Printed in the UK

Random walks and NMR measurements in porous media

Michael Leibig†
The James Franck Institute and Department of Physics, The University of Chicago, 5640 South Ellis Avenue, Chicago, IL 60637, USA

Received 13 July 1992, in final form 19 February 1993

Abstract. This paper studies the relationship between NMR measurements of the magnetization decay in porous media and random-walk problems. The behaviour of this decay can be related to the statistical properties of random walks which interact with the pore–solid interface via perfectly reflecting boundary conditions. An efficient numerical technique measures these statistics using a variable step size random-walk simulation. This technique is applied to three simple models for porous materials. The results indicate that there is a regime of stretched-exponential relaxation of the magnetization for a percolation model.

1. Introduction

Nuclear magnetic resonance (NMR) techniques have shown promise as a tool for understanding the structure of materials. In their classic work, Brownstein and Tarr used NMR relaxation measurements to determine the size of biological cells [1]. They also looked at three simple geometries for pore spaces and calculated the corresponding relaxation curves. Since then there has been much interest in determining the type of structural information that can be discerned from NMR experiments [2–6].

Different types of NMR measurements can be performed on a sample of porous material, and each technique yields different information about the pore structure [2, 6, 3]. The numerical methods that I discuss are most directly applicable to the following NMR experiment. A sample of a porous material is saturated or partially saturated with a fluid which contains an NMR active nucleus. Let the pore volume be written as V, with the pore surface S referring to the boundary between the pore space and the solid material of the sample. The sample is placed in a high magnetic field and acquires a net magnetization in the direction of this external field. The sample is then exposed to a short RF pulse at the Larmor frequency of the active nucleus. This pulse rotates the sample's magnetization away from the direction of the external field [4]. After the initial pulse, the magnetization will, through natural processes, relax back to its original orientation.

There are, of course, many subtle experimental issues associated with actually making these measurements [10, 13]; however, the basic physics of the system is straightforward. The time evolution of any component of the local magnetization density, $m(x, t)$, in the pore volume is described by [31]

$$\frac{\partial m(x,t)}{\partial t} = D\nabla^2 m(x,t) \qquad m(x,0) = M_0$$
$$D\frac{\partial m(x,t)}{\partial n}\bigg|_{x\in S} = -\rho\, m(x,t)|_{x\in S} \qquad m(t) = \int_V m(x,t)\mathrm{d}x \tag{1.1}$$

† Present address: HLRZ KFA-Jülich, Postfach 1913, 52425 Jülich, Federal Republic of Germany.

0305-4470/93/143349+19$07.50

where D is a diffusion constant, M_0 is the magnetization at time $t = 0$ and ρ is the surface relaxation parameter (which may be different for different components of the magnetization) [10]. Experimentally, it is the quantity $m(t)$ that is actually measured. These equations ignore the effect of the decay which occurs in the bulk liquid; it has been shown that this bulk relaxation gives only a trivial exponential prefactor to $m(t)$ [9].

It is straightforward to create a random-walk algorithm whose behaviour is described by equations equivalent to (1.1). Consider N_0 random walkers placed within the pore volume of the sample at $t = 0$. Whenever any of these walker encounters the interface, it is destroyed with a probability q and reflected back into the pore volume with a probability $1-q$. Given these rules, the density of these random walkers, $u(x, t)$, satisfies the following equations:

$$\frac{\partial u(x,t)}{\partial t} = D'\nabla^2 u(x,t) \qquad u(x,0) = N_0/V$$
$$D'\frac{\partial u(x,t)}{\partial n}\bigg|_{x\in S} = -q'u(x,t) \qquad u(t) = \int_V u(x,t)\mathrm{d}x \tag{1.2}$$

where D' is a diffusion constant (which depends on the microscopic size, a, of a single step, the time, τ, for such a step, and d, the dimensionality of space) [21], and q' is a constant determined by the microscopic details of the random-walk algorithm [11, 14]. There is currently some debate over the proper functional form for q' in lattice simulations. Fortunately, the analysis and formalism that I present below do not depend crucially on these details. When making comparisons with experimental observations, I will assume that $q' \approx qa/\tau$, which is the accepted form for small q. The quantity $u(t)$, which corresponds to the measurable quantity $m(t)$ in the magnetization experiment, can be interpreted as the probability that a typical walker will survive to a time t.

The correspondence between $m(t)$ and $u(t)$ suggests a computational method for calculating the decay curve that would be measured for a specific model of a porous material. With the geometry of the pore space encoded into computer memory (e.g. as a set of points in space, or a set of intersection planes), it is possible to implement this partially reflecting random-walk scheme to calculate the function $u(t)$ [11, 14]. The NMR magnetization curve for such a model pore space is then simply given by

$$m(t) = \frac{M_0}{N_0}u(t)\,. \tag{1.3}$$

Unfortunately, this random-walk method suffers from two fundamental problems. The first is that as time passes, the number of times that a typical walker has encountered the surface increases. Since each of these contacts represents a possible termination of the walk, it requires a large number of walks to get good statistics at long times.

The second difficulty is that the passage of time is measured in units of τ, the amount of 'time' required to take one step of length a. Thus, to measure the elapsed time for a specific walk, the trajectory must be made up of steps with this fixed size. This method becomes inefficient when the trajectory of the random walk takes it into the centre of a large void. It takes a very large number of steps for the walk to make significant progress toward the surface.

It is possible to overcome these problems with the numerical methods presented below and there are two facts that motivate this investigation and distinguish it from earlier numerical studies. The first is that the properties of random walks that are either destroyed or reflected at a surface are intimately related to the properties of walks that are always

reflected from that surface. Thus, the partially reflecting random-walk algorithm can be replaced by one that utilizes random walks that live forever.

The second important fact is that it is possible to have a variable step size random walk and still retain time information. Consider a random walker taking a single step of length r. To know the elapsed time for this one step, it is necessary to determine the number of steps that it would have required to make this excursion with steps of length a. This calculation has been done for the case of a continuous random walk [20]. By making use of this result it is possible to determine probabilistically how many small steps would have been required to make the progress that was made by a single large step.

The rest of this paper is organized in the following manner. In section 2, I present the formalism that relates the quantity $u(t)$ to the properties of random walks that are always reflected from the pore surface. Section 3 contains a brief discussion of the numerical method used and then presents results for three simple models for porous media. Section 4 contains some discussion of the applicability of this numerical method to real systems, and an extension of these ideas to a different NMR problem. In appendix A, I describe the relevant details of my implementation of the random-walk scheme discussed in section 3.

2. Formalism

Consider a specific walker labelled by i, moving about the pore volume with the partially reflecting random-walk algorithm described above. Imagine that a record is kept of the total number of steps that this walker has taken since its creation. For each contact with the boundary surface, I define $P_n^i(t)$ as the probability that at time t the ith walker had its nth contact with the boundary. (For a random walk with a fixed step size, the distribution $P_n^i(t)$ is a δ-function in time. I show below that for variable step size walks, $P_n^i(t)$ is a general distribution.) The character of $P_n^i(t)$ will depend on the environment of the walk. A walk which remains in a relatively confined region can quickly accumulate n contacts with the boundary, while a walk which explores a large void requires a large amount of time to accrue n bounces.

The integral $\int_0^t \mathrm{d}t' P_n^i(t')$ is the probability that this walker has bounced n times within a time t. Let the contact at which the ith walk is terminated be denoted as n_i. For $n \leqslant n_i$, $\int_0^\infty \mathrm{d}t' P_n^i(t') = 1$, while this integral is zero for $n > n_i$. I define $u^i(t)$ as the probability that the ith walker is still alive at time t. This can be written as

$$u^i(t) = 1 - \sum_{n=0}^{n_i} \int_0^t \mathrm{d}t' P_n^i(t') \tag{2.1}$$

where I have labelled the first contact with the surface as $n = 0$. I now write the total number of walks that survive to time t as

$$u(t) = N_0 - \sum_{i=1}^{N_0} \sum_{n=0}^{n_i} \int_0^t \mathrm{d}t' P_n^i(t') \,. \tag{2.2}$$

The labelling by i is arbitrary, and thus I choose to sort the data according to the condition $n_1 \leqslant n_2 \leqslant \cdots < n_{N_0}$. Define k_j as the number of walks that died after exactly j contacts with the cluster. Then I may write

$$u(t) = N_0 - \sum_{i=1}^{k_0} \int_0^t \mathrm{d}t' P_0^i(t') - \sum_{i=1+k_0}^{k_0+k_1} \int_0^t \mathrm{d}t' P_1^i(t') - \sum_{i=1+k_0+k_1}^{k_0+k_1+k_2} \int_0^t \mathrm{d}t' P_1^i(t') - \cdots \tag{2.3}$$

where the first term comes from the walks that were terminated on the first contact, the second term comes from walks that were terminated on the second contact, and so on.

Consider the jth term in this series. It is made up of k_j walks that terminated on the jth contact with the surface. Thus, up until this final contact, these walkers behaved just as if they were walkers that were never going to be destroyed. Therefore, I consider a modified random-walk algorithm in which a large number of random walkers are released in the same pore volume and whenever a walker crosses the surface S, it is always reflected. I define $P_n(t)$ as the probability that one of these walks had its nth bounce at time t. Thus the normalization condition is $\int_0^\infty \mathrm{d}t\, P_n(t) = 1$.

The behaviour of these walks as they strike the surface for the jth time should be the same as the behaviour of the k_j walks that are destroyed at this contact. Thus, I write

$$\sum_{l=1+k_0+k_1+\cdots+k_{j-1}}^{k_0+k_1+\cdots+k_j} \int_0^t \mathrm{d}t' P_j^l(t') = k_j \int_0^t \mathrm{d}t'(t') P_n(t') . \tag{2.4}$$

I now use the fact that on average $k_j = N_0 q(1-q)^j$, along with (2.3) and (2.4) to write

$$u(t) = N_0 \left[1 - q \sum_{n=0}^{\infty} (1-q)^n \int_0^t \mathrm{d}t' P_n(t') \right] . \tag{2.5}$$

The quantity in brackets in (2.5) is dependent only on quantities averaged over all random walks which are reflected after every contact with the surface S. Using relation (1.3), I find that the magnetization is

$$m(t) = M_0 \left[1 - q \sum_{n=0}^{\infty} (1-q)^n \int_0^t \mathrm{d}t' P_n(t') \right] . \tag{2.6}$$

Also useful is the time derivative of $m(t)$,

$$\frac{\mathrm{d}m(t)}{\mathrm{d}t} = M_0\, q \sum_{n=0}^{\infty} (1-q)^n P_n(t) . \tag{2.7}$$

Equations (2.6) and (2.7) represent the main results of this section.

It is worth discussing the issue of averaging in somewhat more detail. In studying a problem involving random walks which are destroyed, it may seem counter-intuitive to use statistics derived from a set of walks that are always reflected from S. If some of these walks which never terminate, had been forced to terminate, then clearly some of some of these walks would not contribute to the behaviour at large n. But *which ones would contribute?* The answer is that because the walks which survive are chosen at random, each walk could potentially have contributed. Thus, the statistics of the surviving walks should be independent of the number of walks which survive. In order to get the best statistics, I allow all of the walks to survive.

I have recast the problem of calculating $u(t)$ into determining the set of functions $P_n(t)$. These functions are, of course, interesting in their own right. They are quantities describing the behaviour of a random walk moving in a confined geometry. The true promise of this method, however, is that it may be possible to understand the function $P_n(t)$ in terms of the structural features of the pore geometry or vice versa. If a form for these functions can be derived theoretically, or measured computationally, (2.6) gives the experimentally measurable relaxation curve for such a pore geometry.

3. Numerical results

This section begins with a brief discussion of the computational scheme used to calculate the functions $P_n(t)$. Only the most important ideas are presented here, with more details being provided in the appendix.

$P_n(t)$ is defined as the probability that a walker which is started with equal probability anywhere in the pore volume will have its nth encounter with the pore surface at time t. This probability is averaged over all possible trajectories available to the walker.

A standard trick which increases the efficiency of a random-walk algorithm is to use a variable step size random walk [22]. By this scheme, when a walker is far from an interface, it takes larger steps, taking short steps of the minimal size, a, only when it is near to a surface. However, in taking these large steps, I need to know how many short steps would have been required to cover the distance of the larger step. Because I am interested in averaging over all random-walk trajectories, it is the distribution of possible elapsed times that is of interest. Thus, the variable step size walk actually provides more information with fewer walkers than the standard fixed step size algorithm.

In the continuum limit (i.e. $a \to 0$, $\tau \to 0$, $D' = a^2/\tau d = \text{constant}$), there is a discrete solution for the problem of the elapsed time distribution for variable step sizes [20]. For spatial dimension $d = 2$, the probability, $p_r(t)$, that a random walk will travel a linear distance r in time t is

$$p_r(t) = \frac{2D'}{r^2} \sum_{k=1}^{\infty} \frac{\zeta_{0,k} \exp(-\zeta_{0,k}^2 D' t / r^2)}{J_1(\zeta_{0,k})} \tag{3.1}$$

where $J_n(x)$ is the Bessel function of order n, and $\zeta_{0,k}$ is the kth zero of $J_0(x)$. (It is possible to calculate $p_r(t)$ for $d > 2$, but in this work, for simplicity, I consider only two-dimensional systems.) Unfortunately, (3.1) is valid only for a continuous random walk. For large r, however, this expression provides a good approximation to the discrete probability distribution.

Equation (3.1) gives the probability distribution for the elapsed time of a single step of length r. In order to calculate the distribution of elapsed time for a collection of such steps, it is simply a matter of performing a series of convolutions of many functions of the form of (3.1) with the values of r being determined by the specific trajectory of the walker. The resulting convolution from all steps up to the nth contact gives the function $P_n^i(t)$. Averaging over all such walks, I determine $P_n(t)$.

I now turn to the results of a study of three different geometric models for porous materials. For each model, I discuss the observed $P_n(t)$ and, where possible, consider the NMR decay that each pore geometry would produce. The first model pore space is the interior of a circle. The trivial nature of this geometry allows for comparison with exact results and illustrates the basic behaviour for an isolated pore.

The second model is a set of identical circular pores connected to one another with narrow channels. This relatively minor change from an isolated pore results in drastic changes in $P_n(t)$. Additionally, since the behaviour of random walks is well understood for both the circular pore and in the narrow channel separately [19], this model should lend itself to analytic calculation.

The third model for a porous material is a percolation cluster. Percolation is an important problem in condensed matter physics [25], and the functions $P_n(t)$ may provide a fruitful tool for understanding its structure. As a model for porous media, it also captures the flavour of the random grain structure of many real porous samples, and there have been

experimental measurements of porous materials that have shown percolation-like behaviour [16].

These models are not intended to serve as exact representations of the microstructure for a physical porous medium. The actual geometry of a real porous material is very sample specific. There is a bewildering variety of influences which contribute to the formation of real rocks, and each of these factors affects the microscopic details of the pore surface [18]. It is not my goal to create a perfectly accurate physical description for one specific sample and then measure the function $P_n(t)$ for it. The purpose of this numerical study is to illustrate the geometrical features that affect the function $P_n(t)$, and more importantly, the relaxation curve $m(t)$.

In the analysis of the functions $P_n(t)$, I will show two different types of results for each curve. The first is derived from the moments of each distribution. For each model pore space I plot as a function of n, the average elapsed time, $\langle t\rangle_n$, the standard deviation for the distribution, $\langle\sigma\rangle_n$, and the skewness of the distribution, $\langle\eta\rangle_n$. The skewness involves the third moment of the distribution and reflects the symmetry of the distribution about the average. A positive skewness indicates that the tail of the distribution is much broader above the mean than below. The opposite is true for a negative skewness.

I also show for each pore the actual functions $P_n(t)$. For large n, these curves take on the scaling form

$$P_n(t) = \frac{1}{\langle\sigma\rangle_n} \exp\left[-F\left(\frac{(t-\langle t\rangle_n)}{\langle\sigma\rangle_n}\right)\right] \tag{3.2}$$

where $F(x)$ is some function characteristic of each model. In order to display the behaviour of $F(x)$, it is convenient to plot $\log(\langle\sigma\rangle_n P_n(t))$ versus $(t-\langle t\rangle_n)/\langle\sigma\rangle_n$. For the circle and percolation, I am able to make quantitative statements about the function $F(x)$, as well as to calculate its implications for the long-time behaviour of the magnetization decay.

All of the data shown below are averages over 10 000 random walkers. For calculating the moments, I followed these walks up to $n_{\max} = 10\,000$ bounces. In measuring the full functions $P_n(t)$, I only calculated up to $n_{\max} = 1000$. The results are reported assuming $a = 1$ and $\tau = 1$.

3.1. The circle

The simplest possible model for a pore space is the interior of a circle. This problem was taken up by Brownstein and Tarr, and the behaviour of the magnetization is well understood. This makes it an ideal testing ground for the exploration of the relationship between the functions $P_n(t)$ and the magnetization decay.

Numerical simulations were performed on circles of various sizes; here I present the results for a circle with a radius $R = 10a$. The behaviour of the average time, the standard deviation and the skewness are shown in figures 1 and 2. All three of these quantities have been plotted on a logarithmic scale to show their power-law behaviour.

For large n, the average time $\langle t\rangle_n \approx Rn$. It is possible to show [20] that for a random walk starting a distance b from the surface of a circle, the average time, $\bar{t}$, at which that walker encounters the circle is

$$\bar{t} = bR(1 - b/2R) \tag{3.3}$$

where I have used the fact that in my simulations the walker's diffusion constant $D' = \frac{1}{2}$. Before the first contact with the circle, the random walkers begin with a uniform distribution

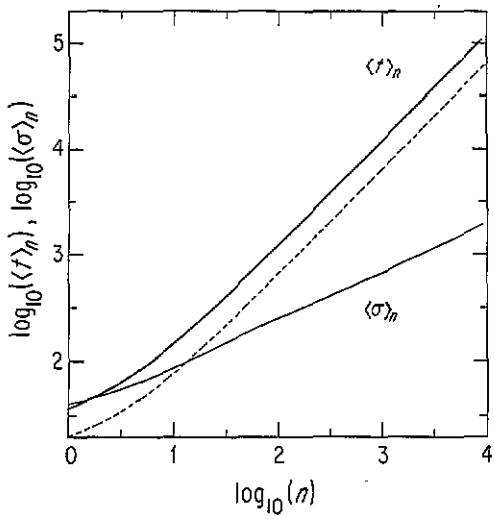

Figure 1. Average and standard deviation of $P_n(t)$ for the random walks inside a circle. The broken curve is the exact result for a continuum random walk.

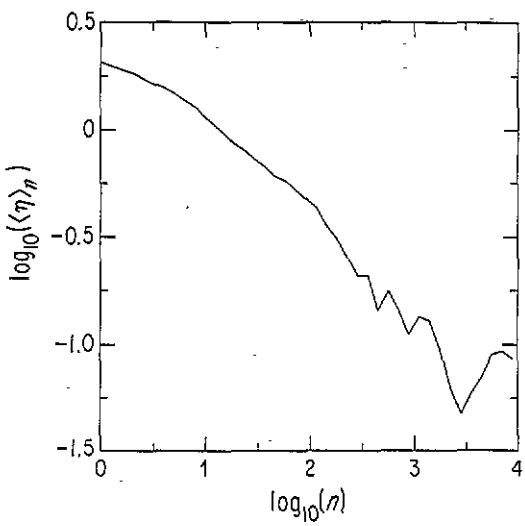

Figure 2. Skewness of $P_n(t)$ for the circle. The curve seems to indicate a power-law-like decay. The high level of noise for large n is a result of the sensitivity of higher moments to outliers.

inside the circle. Thus, to determine $\langle t\rangle_0$, I integrate over all possible starting radii. I find that

$$\langle t\rangle_0 = R^2/4\,. \tag{3.4}$$

After the first bounce, the walkers always start a distance $b' \approx 0.75$ from the edge of the circle (the reason that $b' < 1$ is discussed in the appendix). Thus, I have

$$\langle t\rangle_n = R^2/4 + nRb'(1 - b'/2R)\,. \tag{3.5}$$

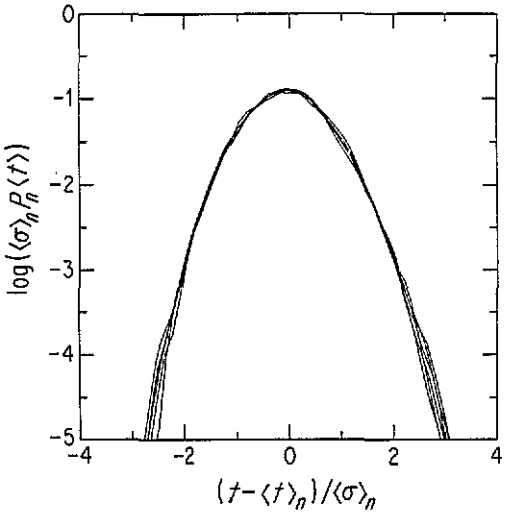

Figure 3. $P_n(t)$ for circle for $n = 316, 398, 501, 630, 794, 1000$. The data have been collapsed to show the form of $F(x)$.

The curve (3.5) is also plotted in figure 1. Note that the theoretical curve is displaced below the numerical result. This shift exists because (3.5) is for a continuous random walk, and diffusion on the smallest scales happens faster for continuous walks than for discrete walks. The two curves can be brought together by choosing the unit of time for the continuous random walk to be $1.8\,\tau$.

Figure 1 shows that at large n the standard deviation increases as $n^{1/2}$. This can be understood by considering the central limit theorem, which states that if I choose n times at random from a fixed distribution, then asymptotically the distribution that describes my total after n draws will be a Gaussian [27]. This distribution will have a mean that goes linearly in n and a standard deviation that increases as $n^{1/2}$. After the first bounce, this applies exactly to this random-walk problem. There is some function that describes the distribution of elapsed times between successive contacts with the circle. Each time a random walk moves from bounce n to $n+1$, it is taking a sample from that distribution function. Thus, the central-limit theorem should apply to $P_n(t)$ in the limit of large n.

Also, notice that the skewness seems to show a power-law decay to zero. This implies that the distribution is becoming more symmetric as n increases, as it should if this function is becoming a Gaussian.

The actual functions $P_n(t)$ are shown in figure 3. The data have been collapsed as described above to show the form of $F(x)$ for the circle. I assume the form $F(x) \approx A + B|x|^\alpha$ near $x = 0$. The difficulty in determining α from the data arises because of the inherent noise which masks the behaviour near $x = 0$, and because the usable data extends only to $x = 3$. To find the power law, I subtract the value at the maximum from $F(x)$, and then plot the resulting function on a log–log scale. The results for $x < 0$ are shown in figure 4. From the central-limit theorem argument, I expect that $\alpha = 2$, and the curves show good agreement with this in the large-n limit.

Finally, consider the long-time behaviour of the magnetization implied by the Gaussian form for $P_n(t)$. For long times, it will be the large-n terms that contribute and I have from (2.7)

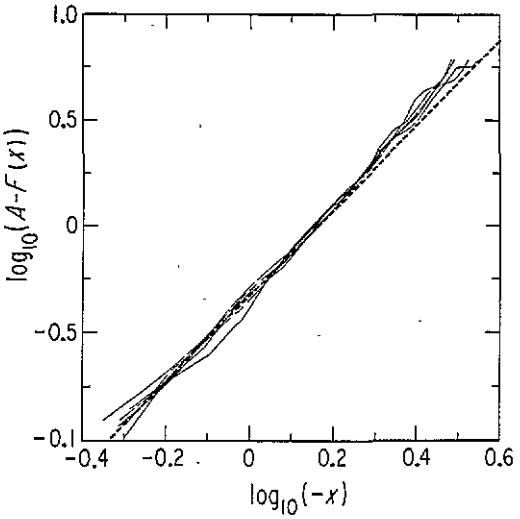

Figure 4. Power-law behaviour for $F(x)$ for $x < 0$. The value of $A = -0.90$. The broken lines show the behaviour for $F(x) = A + Bx^2$.

$$\frac{dm(t)}{dt} = M_0\, q \sum_{n=0}^{\infty} \frac{A'}{n^{1/2}} \exp(-nq'' - (t - Rn)^2/Cn) \tag{3.6}$$

where $q'' = -\log(1-q) > 0$, with A' and C constants. Ignoring logarithmic corrections, and converting the sum into an integral, I can evaluate (3.6) by the method of steepest descent. I then find that for large times,

$$m(t) \doteq M_0' \exp(-t/T) \tag{3.7}$$

where M_0' and T are constants. This is exactly the form for the long-time decay of the magnetization in a circular geometry [1]. Thus, this Gaussian form for $P_n(t)$ leads to simple exponential decay.

3.2. Connected circles

The next level of difficulty is the case of connected pores. I choose to study a system of identical circular pores connected by long narrow channels. Physically, this might model a sample in which the voids in a rock are connected by long cracks. I have simulated this by considering a single pore of radius R connected to two channels on opposite sides, as shown in figure 5. I then impose periodic boundary conditions, and this becomes an infinite system of pores. The three important length scales are the radius R of the pore, the length L of the channel, and the width W of the channel. The results shown below are for $R = 20a$, $L = 40a$, and $W = 5a$.

The results for the average, standard deviation and skewness are shown in figures 6 and 7. Also shown are the results for a single circular pore with the same value for R. The $\langle t \rangle_n$ becomes linear for large n, but the curve is lower than for a single pore. Thus, the channel decreased the effective radius of the pore.

The $\langle \eta \rangle_n$ is plotted versus $\log(n)$ in figure 7. This curve indicates that the asymptotic state for the distribution is asymmetric, with a broad tail at short times. The region $10 \leqslant n \leqslant 150$ suggests that the curve has a regime in which $\langle \eta \rangle_n = K_0 + K_1 \log(n)$. Doing a least-square fit, I find $K_0 \approx 3.0$ and $K_1 \approx -0.6$.

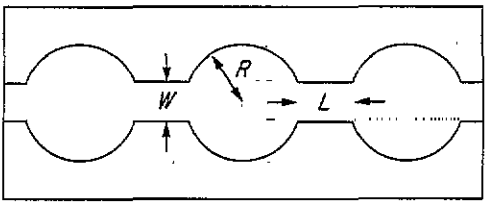

Figure 5. Circular pores with connecting narrow channels. The pores are of radius R and the channels have a length L and a width W.

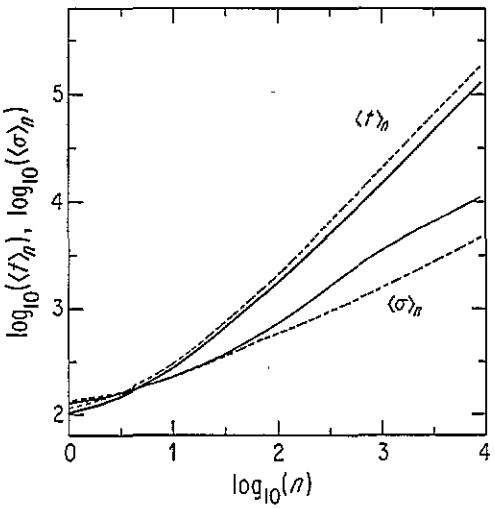

Figure 6. Average and standard deviation of $P_n(t)$ for the circular pores with connecting channels. The broken curves are the results for an isolated circular pore with the same value of R.

The gross behaviour of the random walkers is evident in $P_n(t)$. In figure 8, I show the short-time behaviour of these functions. The broad peak is associated with walkers which start in the large pore. The peak at short times is due to the random walks that initially find themselves in the narrow channel. It will take walks which remain in this channel little time to accumulate n bounces. It is also evident that at some $n \sim 500$ this peak can no longer be distinguished from the tail of the distribution caused by walks that have visited the pore. This indicates that almost all of the walks that started in the channel have visited the pore at least once and have had their individual probability distribution smeared out by the long trajectories available in the large pore.

When would this behaviour of a strong peak which dies out slowly be manifested in a general pore structure? An initial strong peak at a small time is characteristic of any structure which has one dimension that is small. The fact that it takes several hundred bounces for this peak to disappear is due to the long dimension of the channel. Had these random walks started in a small circle which had relatively easy access to a neighbouring large pore, this peak would have died out at much smaller values of n. Thus, long-lived, short-time peaks should be characteristic of either small pores that are very isolated from their surroundings, or from structures that have very large length-to-width ratios.

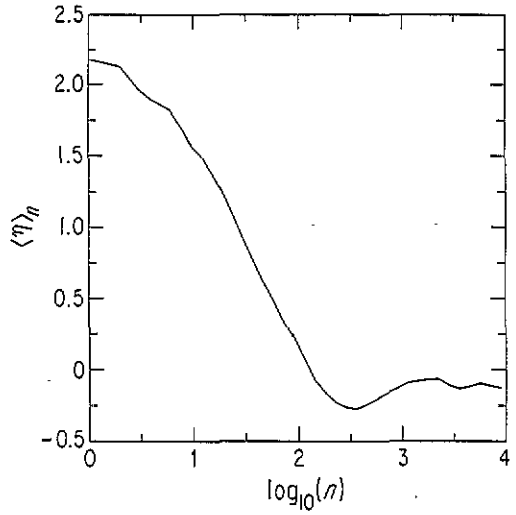

Figure 7. Skewness of $P_n(t)$ for circular pores with connecting channels. The value for large n is negative, indicating a broader tail for shorter times. This curve also appears to have a linear regime from $10 \leqslant n \leqslant 150$.

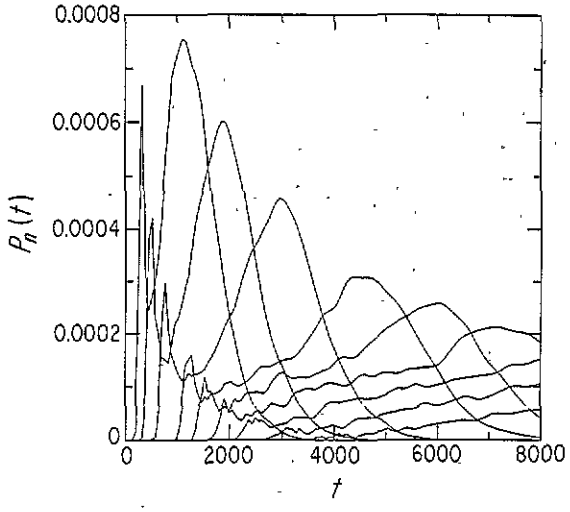

Figure 8. $P_n(t)$ for short times. The curves shown are for $n = 63$, 100, 158, 251, 316, 398, 501, 630, 794. The small peak at short times is indistinguishable from the tail of the broad peak after $n = 501$.

Figure 9 shows the collapsed form of the $P_n(t)$. There is a a clear asymmetry in the distribution. It may seem surprising that $F(x)$ does not possess the simple parabolic form for its asymptotic state. Unfortunately, the central-limit theorem does not apply to this geometry. The difference between this case and the circle is that here the random walk is not always sampling from the same distribution. Walkers in the channel have a very different distribution for the elapsed time between bounces than do walkers in the large pore.

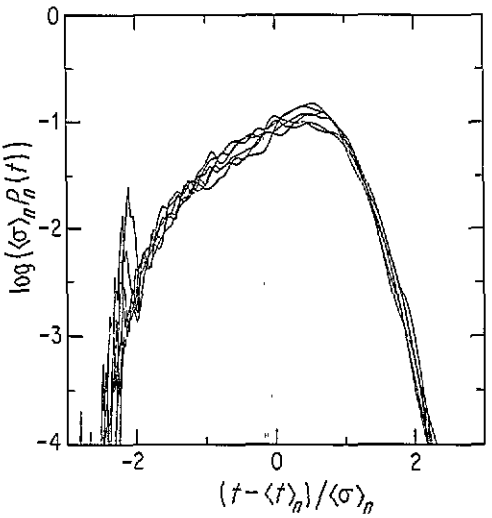

Figure 9. $P_n(t)$ for circular pores with channels $n = 316, 398, 501, 630, 794, 1000$. The data has been collapsed to show the behaviour of $F(x)$. The curves are highly asymmetric, and the small peak is moving to the left for larger n.

3.3. Percolation

The final model that I wish to consider is the pore geometry of continuum percolation [28]. The model is generated by placing circles at random in a square with periodic boundary conditions. Figure 10 shows the specific realization of the circles used in the results shown below. The square has an edge of length $L = 100a$, and each circle has a radius $R = 3a$. The pore volume is the entire region not covered by the circles. There is a well-connected region which extends from one end of the square to the other, and thus the region complementary to the circles has a 'percolating cluster', and the pore space is above the percolation threshold.

The results for the average, standard deviation and skewness are shown in figures 11 and 12. In the large-n limit, $\langle t\rangle_n$ seems to be slowly approaching a linear behaviour, and gives an effective radius of the pores of $R \approx 10a$. In the region $100 < n < 10000$, a least-square fit indicates that $\langle t\rangle_n \sim Rn^{0.97}$.

The $\langle\sigma\rangle_n$ also displays a region of anomalous power-law behaviour. If I write $\langle\sigma\rangle_n \sim n^{\beta}$, then I find that for percolation, $\beta = 0.71 \pm 0.02$. The implications of this power-law behaviour will be discussed below. The $\langle\eta\rangle_n$ is plotted versus $\log(n)$. Fitting the linear region $150 \leqslant n \leqslant 7000$ to the form $\langle\eta\rangle_n = K_0 + K_1 \log(n)$, I find $K_0 \approx 2.7$ and $K_1 \approx -0.5$. Note also that all of these moments seem to display a clear cut-off in the scaling behaviour at $n \approx 7000$.

In figure 13, I show the form of $P_n(t)$ for this model. I have collapsed the data to attempt to determine the function $F(x)$. There are two behaviours which are of interest. The first is the cross-over at very small values of x. It may be that this curve becomes constant for large negative x.

Also unusual is that in the broad peak there seems to be different behaviour above and below $x = 0$. I assume that near $x = 0$, I have $F(x) \approx A + B|x|^{\alpha_\pm}$, where the plus and minus indicate different values for positive and negative values of x. Figure 14 shows the results from subtracting the value of A, and plotting the resulting curves on a log–log scale for $x < 0$. For small negative x, I find that $\alpha_- \approx 1.6$. A similar plot for $x > 0$ shows

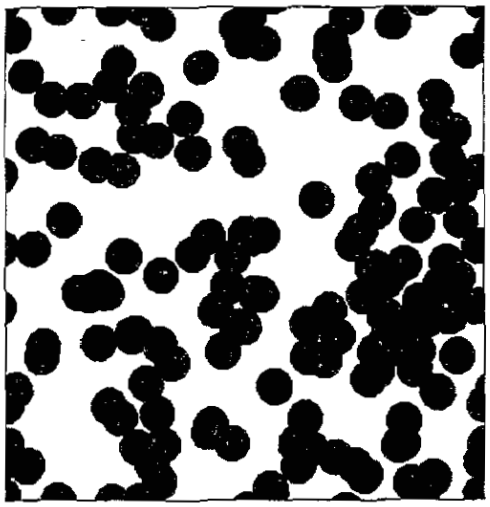

Figure 10. Continuum percolation model for porous material. There are 150 circles of radius 3 on a 100 × 100 square. The random walks move in the region exterior to the circles.

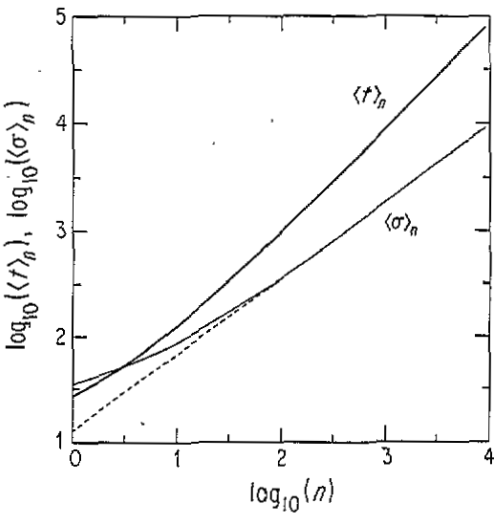

Figure 11. Average and standard deviation of $P_n(t)$ in the percolation model. The broken curve has the same slope as the power-law behaviour in $\langle\sigma\rangle_n$.

that $\alpha_+ \approx 2.3$. For $x > 0$, it was not clear that an asymptotic state had been reached, and the true exponent α_+ may be lower than reported here. Fortunately, the behaviour of the magnetization is quite insensitive to the behaviour above $x = 0$.

These power-law behaviours have interesting consequences for the magnetization decay, $m(t)$. Consider the time derivative of the magnetization, assuming the power-law form for $F(x)$,

$$\frac{\mathrm{d}m(t)}{\mathrm{d}t} = M_0\, q \sum_{n=0}^{\infty} \frac{A'}{n^{\beta}} \exp(-nq'' - (t - Rn^{\delta})^{\alpha_\pm}/Cn^{\beta\alpha_\pm}) \tag{3.8}$$

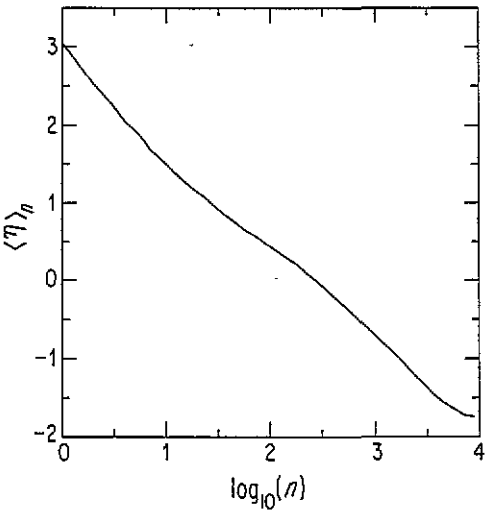

Figure 12. Skewness of $P_n(t)$ for the percolation model. The negative value for large n indicates a broad tail for small t. The curve also seems to display a linear behaviour for $150 \leqslant n \leqslant 7000$.

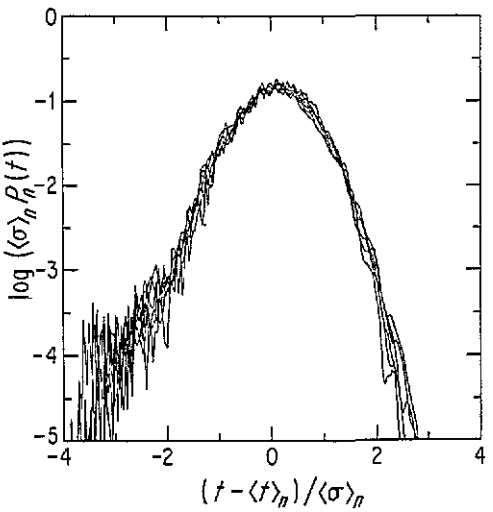

Figure 13. $P_n(t)$ for the percolation model for $n = 316, 398, 501, 630, 794, 1000$. The data has been collapsed to show $F(x)$. The data suggests that $F(x)$ may become constant for large negative x.

where I have assumed that $\langle t \rangle_n = Rn^{\delta}$, and the constants are defined as in (3.6). I again turn this sum into an integral and evaluate it by steepest descent. In the long-time limit, I obtain a magnetization of the form

$$m(t) = M_0' \exp(-(t/T)^{\psi}) \tag{3.9}$$

where M_0' and T are constants, and I have ignored logarithmic corrections. The value of the exponent is given by

$$\psi = \frac{\alpha_-}{\alpha_- \beta + 1}. \tag{3.10}$$

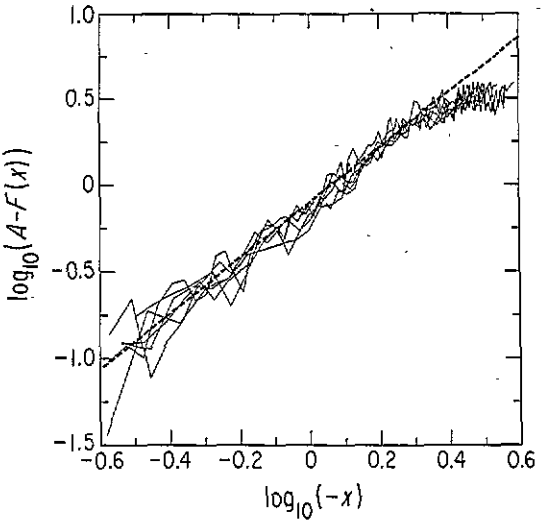

Figure 14. Power-law behaviour of $F(x)$ for $x < 0$ in percolation model. The value used for $A = -0.85$. The broken line shows the behaviour for $F(x) = A + B|x|^{1.6}$. Again the data suggests that $F(x)$ becomes constant for large negative x.

For the case of percolation, this gives $\psi \approx 0.75$.

The long-time limit is, however, a serious restriction on the experimental observability of such behaviour. To be observed, there must be sufficient magnetization remaining in the pore volume. At $n = 1/q''$, 63% of the initial walkers would have been terminated. In the calculation that gives (3.10), the long-time limit means that this stretched exponential behaviour will be seen only for $t > t^*$, where $t^* \sim (1/q'')^{\chi}$. The exponent χ is given by

$$\chi = \frac{\delta}{1 - \alpha_-(\delta - \beta)}. \tag{3.11}$$

The natural observability condition is that $\chi \leqslant 1$. For percolation, $\chi \approx 1.6$.

There is also a long-time cut-off time when this stretched exponential will no longer be observed. This occurs when either the maximum of the exponent in (3.8) moves outside the power-law regime of the function $F(x)$, or when the anomalous power-law behaviour disappears.

Finally, it is worth emphasizing the relationship between the numerical results from the random-walk simulation and the determination of the magnetization decay. The computational study yields information about the form of the functions $P_n(t)$. This form was then used in the series (3.8), and that series was then evaluated analytically. This analysis lead to a the prediction for the magnetization of the form given by (3.9) and (3.10). This illustrates the approach that must be taken for each specific geometry—first determine the behaviour of $P_n(t)$ and then evaluate analytically the series (2.7) to determine the magnetization decay. This approach is, in spirit, very similar to a method by which the double-layer impedance for fractals was determined by using random-walk methods [32].

4. Discussion

In this work, I have described a new formalism with which to consider the problem of magnetic relaxation in porous media. This formalism suggests a natural numerical scheme

to measure the behaviour of model systems, and I have discussed ways to make this method a practical computational tool. Finally, I applied this numerical method to three systems and discussed the resulting behaviours.

By far the most exciting implication for real systems is the observed mechanism for a stretched exponential relaxation, a behaviour that is common in measurements of the magnetization in real rocks [17, 8]. Equation (3.10) and the analysis that leads to it, does not depend on the percolation geometry, only on the existence of the power-law behaviour of $P_n(t)$. This suggests that the stretched exponential behaviour is more than an interesting way to plot experimental data, but reflects the fundamental behaviour of the magnetization decay. The next step is to understand under what circumstances the required power-law behaviour will be observed in $P_n(t)$.

This method is, of course, still a long way from being a useful technique for characterizing a porous material. The success of this work comes from recasting the calculation of $m(t)$ into the problem of calculating $P_n(t)$, this latter quantity being much more amenable to analytical and numerical study.

The general method of calculating the time behaviour for a variable-step-size random walk may have interesting applications to other NMR methods used to study porous media. In recent work on pulsed field gradient methods [7], an important parameter is an effective diffusion coefficient for the system. For a particular pore geometry, this coefficient is proportional to the mean-square displacement of the walker at time t. The numerical method presented here should easily generalize to calculate the distance from the walker's initial position as well as the elapsed time for the walk.

Acknowledgments

I would like to thank T C Halsey for his suggestion to study this problem, his help with the manuscript and fruitful discussion throughout this project. I would also like to acknowledge R A Goldstein for his original insights and his notes regarding some of the material on random walks. Finally, I would like to acknowledge useful discussion with B Duplantier, R Blumenfeld, P Mitra, W Halperin, K McCall, L Schwartz and P Le Doussal. Financial support for this work was provided by the Materials Research Laboratory.

This work is presented as a thesis to the Department of Physics, The University of Chicago, in partial fulfillment of the requirements for the PhD degree.

Appendix. Calculating $P_n(t)$: Details of the Implementation

In this appendix, I present further information about the numerical algorithm that I described briefly in section 3. In writing an actual program which performs the random walk and calculates the functions $P_n(t)$, there are many important details which are not described here. I discuss only those pieces of information which serve to clarify what is actually being calculated in section 3, and which may help readers who wish to use some of these ideas in their computational studies.

There are two distinct computational processes involved. The first is performing a large number of off-lattice random walks with variable-step-size. The second is transforming the step size information from these walks into the functions $P_n(t)$. I begin with a discussion of the random-walk simulation. Recall from above that my calculations are for a two-dimensional off-lattice random walk, and for this I choose a minimum step of length 1 which takes a time 1. Such an algorithm has a diffusion constant $D' = \frac{1}{2}$. The pore surface

is represented by a discrete set of points, with the distance between neighboring points always less than 1. The simulation then treats these points as the centres for a set of circles with unit radius.

When a walker strikes the surface of one of these small circles, the walk is reflected. The simplest way to simulate this reflection is to return the walker to its position before the step was taken. Even though the step is taken back, the total elapsed time for the walk is still incremented by one—the random walk behaves like a 'myopic' ant [26]. Because the step is taken back, the walker will not always end up a fixed distance away from the surface. This distance will always be less than one, depending on how far the walk is from the surface at the start of its step. With sufficiently large number of walks, the variation in this step-back distance becomes unimportant and the overall behaviour is described by some effective step length.

The rest of the variable step size random-walk algorithm follows conventional methods [22], and I now turn to the numerical processing involved with calculating the functions $P_n(t)$. From (3.1), it is straightforward to calculate numerically the functions $p_r(t)$ for all the different step sizes that the random walk may take. Consider s steps of length r taken between successive contacts of the walk with the pore surface. The contribution of these steps to $P_n^i(t)$ will be from s convolutions of $p_r(t)$ with itself, which I write as $p_r^s(t)$. These self-convolution integrals need only be done once, and then stored for later use. To actually perform these convolution integrals, it is best to do them using a fast fourier transform (FFT) method [24].

The program which actually calculates $P_n^i(t)$ then performs convolutions of these various functions $p_r^s(t)$. The choice of which functions to convolve is the information provided by the random-walk simulation. Each $p_r^s(t)$ is successively convolved with the function which is the probability distribution resulting from all of the previous steps in the walk. After all the steps up to a given contact have been process, the computer has generated $P_n^i(t)$ for that walker.

In order to avoid performing FFTs on excessively long functions, I use the hierarchical data structure shown in figure A1. Each array has a maximum length of L_0. At the bottom of the hierarchy, each element of the array represents a length of time 1. Going up each level in the hierarchy, the amount of time falling into each array element increases by a factor of T_0. As each new function $p_r^s(t)$ contributes, it is convolved with the function occupying the bottom level of the hierarchy. As a result of these convolutions the function in the lowest level increases in size. Eventually it becomes impossible for the next $p_r^s(t)$ to be convolved into the lowest array. When this happens, the function that is in the bottom array is compressed in time by the factor T_0, and is then convolved with the array which is above it in the hierarchy. Once this old function is convolved into the array above, the new $p_r^s(t)$ is placed into the bottom array, and the process is started again. With this procedure, eventually the function in the second level of the hierarchy will grow beyond a length L_0. This second array is then compressed by a factor T_0, and convolved with the function above it. This can be done *ad infinitum*, creating new levels as the total time of the walk is increased. With this hierarchical scheme, FFTs are performed on arrays which are never longer than L_0.

To determine the $P_n^i(t)$ for a specific n, the function in each level must be compressed and convolved with the function directly above it, beginning with the bottom of the hierarchy and continuing to the top. At the end of this procedure, the function which occupies the top of the hierarchy is $P_n^i(t)$. This function is then averaged with the other values of $P_n^i(t)$ which were measured from different random walks. Once this average over all walks is performed, I have $P_n(t)$.

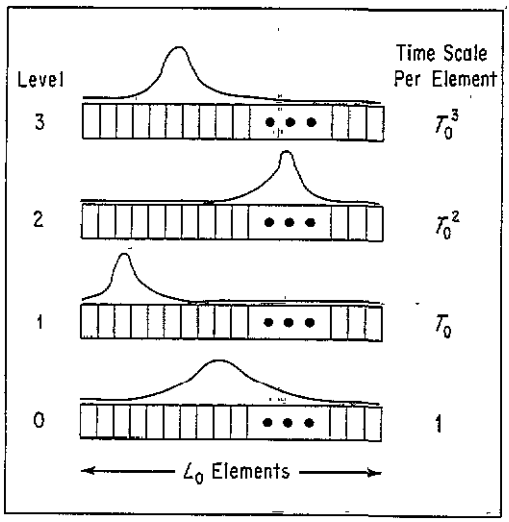

Figure A1. Hierarchical data structure for calculating $P_n(t)$. Each array has L_0 elements. At the bottom of the hierarchy, the time scale for each array element is 1. The time scale associated with an element of the array increases by a factor of T_0 at each level of the hierarchy. Whenever a function gets too long to be contained in its current level, the function is contracted by a factor of T_0 and convolved into the array above it.

With this scheme for calculating $P_n(t)$ it required roughly 20 times more CPU time to process all of the convolutions than to perform the random walks. This suggest that doing simulations to measure $P_n(t)$ for three-dimensional models should not take much more real time than was required for two dimensions. Working in three dimensions will slow down the random-walk part of this procedure, but the convolutions are what determine the overall processing time.

Finally, I would like to mention that it is possible to calculate exactly the moments of the functions $p_r(t)$ in closed form. Thus, when calculating the moments of $P_n(t)$ it is not necessary to do any convolution at all. It is for this reason that the results for the moments are shown up to a much larger value of n.

References

[1] Brownstein K R and Tarr C E 1979 *Phys. Rev.* A **19** 2446
[2] Lipsicas M, Banavar J R and Willemsen J 1986 *Appl. Phys. Lett.* **48** 1544
[3] Wayne R C and Cotts R M 1966 *Phys. Rev.* **151** 264
Robertson B 1966 *Phys. Rev.* **151** 273
[4] Farrar T C 1989 *Pulse Nuclear Magnetic Resonance Spectroscopy* (Chicago, IL: Farragut Press)
[5] Timur A 1969 *J. Petro. Tech.* **21** 775
Loren J D *Petro. J. Tech.* 1972 **24** 923
[6] Mitra P P and Sen P N 1992 *Phys. Rev.* B **45** 143
[7] Mitra P P, Sen P N, Schwartz L M and Le Doussal P *Phys. Rev. Lett.* to be published
[8] Halperin W P, D'Orazio F, Bhattacharja S and Tarczon J C 1989 *Molecular Dynamics in Restricted Geometry* ed J Klafter and J M Drake (New York: Wiley)
[9] Wilkinson D J, Johnson D L and Schwartz L M 1991 *Phys. Rev.* B **44** 4960

[10] D'Orazio F, Bhattacharja S, Halperin W P, Eguchi K and Mizusaki T 1990 *Phys. Rev.* B **42** 9810
Bhattacharja S, D'Orazio F, Tarczon J C, Halperin W P and Gerhardt R 1989 *J. Am. Ceram. Soc.* **72** 2126
[11] Mendelson K S 1990 *Phys. Rev.* B **41** 562
[12] McCall K R, Johnson D L and Guyer R A 1991 *Phys. Rev.* B **44** 7344
[13] D'Orazio F 1990 Geometrical and physical characterization of porous materials by nuclear magnetic resonance techniques *PhD thesis* Northwestern University
[14] Banavar J R and Schwartz L M 1987 *Phys. Rev. Lett.* **58** 1411
Banavar J R and Schwartz L M 1989 *Molecular Dynamics in Restricted Geometries* ed J Klafter and J M Drake (New York: Wiley)
[15] Korringa J, Seevers D O and Torrey H C 1962 *Phys. Rev.* **127** 1143
[16] Thompson A H Katz A J and Raschke R A 1987 *Phys. Rev. Lett.* **58** 29
[17] Dashen R, Day P, Kenyon W, Straley C and Willemsen J *Physics and Chemistry of Porous Media II: AIP Conf. Proc.* vol 154 ed J R Banavar, J Koplik and K W Winkler (New York: American Institute of Physics)
[18] North F K 1985 *Petroleum Geology* (Winchester, MA: Allen and Unwin)
[19] Halsey T C and Leibig M 1991 *Europhys. Lett.* **14** 815
[20] Goldstein R E, Halsey T C and Leibig M 1991 *Phys. Rev. Lett.* **66** 1551
[21] Chandrasekhar S 1943 *Rev. Mod. Phys.* **15** 1
[22] Meakin P 1985 *J. Phys.* A **18** L661
[23] Prudnikov A P, Brychkov Y A and Marichev O I *Integrals and Series* vol 2 (New York: Gordon and Breach)
[24] Press W H, Flannery B P, Teukolsky S A and Vetterling W T 1986 *Numerical Recipes: The Art of Scientific Computing* (Cambridge: Cambridge University Press)
[25] Zallen R 1983 *Percolation Structures and Processes (Annals of the Israel Physical Society 5)* ed G Deutscher, R Zallen and J Adler (Bristol: Hilger)
[26] Mitescu C D and Roussenq J 1983 *Percolation Structures and Processes (Annals of the Israel Physical Society 5)* ed G Deutscher, R Zallen and J Adler (Bristol: Hilger)
[27] Mathews J and Walker R L 1970 *Mathematical Methods of Physics* (Reading, MA: Addison-Wesley)
[28] Gawlinski E T and Stanley H E 1981 *J. Phys.* A **14** L291
[29] Halsey T C and Leibig M 1990 *J. Chem. Phys.* **92** 3756
[30] Leibig M and Halsey T C, unpublished
[31] Torrey H C 1956 *Phys. Rev.* **104** 563
Cohen M H and Mendelson K S 1982 *J. Appl. Phys.* **53** 1127
[32] Halsey T C and Leibig M 1991 *Ann. Phys.* **219** 109
Meakin P and Sapoval B 1991 *Phys. Rev.* A **43** 2993